Clays and Clay Minerals, Vol. 63, No. 3, 145–162, 2015.

SALT DIFFUSION THROUGH A BENTONITE-POLYMER COMPOSITE

GRETCHEN L. BOHNHOFF[1] AND CHARLES D. SHACKELFORD[2,*]

[1] Department of Civil & Environmental Engineering, 1 University Plaza, University of Wisconsin-Platteville, Platteville, Wisconsin 53818-3099, USA

[2] Department of Civil and Environmental Engineering, 1372 Campus Delivery, Colorado State University, Fort Collins, Colorado 80523-1372, USA

Abstract—Bentonites are commonly used as chemical containment barriers to minimize liquid flow and contaminant transport. However, chemicals can adversely affect bentonite performance to the extent that modified bentonites have been developed to improve chemical resistance relative to traditional (unmodified) bentonites. The present study focused on the diffusion of potassium chloride (KCl) through a bentonite-polymer composite, or BPC, that was known to behave as a semipermeable membrane. Specifically, the effective diffusion coefficients, D^*, for chloride (Cl^-) and potassium (K^+) were measured and correlated with previously measured membrane efficiency coefficients, ω, for the BPC. The values of D^* at steady-state for chloride (D^*_{ss,Cl^-}) and potassium (D^*_{ss,K^+}) decreased as the ω values increased. The decrease in D^*_{ss,Cl^-} and D^*_{ss,K^+} was approximately a linear function of $(1 - \omega)$, which is consistent with previous research performed on unmodified Na-bentonite contained within a geosynthetic clay liner (GCL). In contrast to the previous GCL tests, however, D^*_{ss,Cl^-} values for the BPC generally were greater than the D^*_{ss,K^+} values, and the differences between D^*_{ss,Cl^-} and D^*_{ss,K^+} decreased as KCl concentration increased. The apparent discrepancy between D^*_{ss,Cl^-} and D^*_{ss,K^+} is consistent with excess sodium (Na^+) in the BPC prior to testing and the requirement for electroneutrality during testing. Also, despite an apparent linear trend in diffusive mass flux for K^+, lack of agreement between the ratio of the diffusive mass flux of K^+ relative to that for Cl^- as required on the basis of electroneutrality at steady state suggested that steady-state diffusive mass flux for K^+ had probably not been achieved due to continual K^+-for-Na^+ cation exchange. Nonetheless, the excess Na^+ and bentonite modification did not affect the fundamental correlation between D^* and ω, which requires that D^* approaches zero as ω approaches unity ($D^* \rightarrow 0$ as $\omega \rightarrow 1$).

Key Words—Chemico-osmosis, Clay Membranes, Diffusion, Electroneutrality, Geosynthetic Clay Liner, Polymer-modified Bentonites, Semipermeable Membrane Behavior, Sodium Bentonite.

INTRODUCTION

Bentonites are high swelling, clay-rich, natural materials which consist primarily of smectite-group minerals such as montmorillonite. Bentonites are commonly used in chemical containment barriers to minimize liquid flow and contaminant transport. Examples of applications include *in situ* vertical cutoff walls for control of groundwater, engineered (*e.g.* compacted) barriers (liners) for primary waste containment (*e.g.* landfills, wastewater ponds, manure lagoons, nuclear storage, *etc.*) and secondary containment in tank farms, and seals in monitoring and water supply wells (Estornell and Daniel, 1992; Evans, 1994; Kajita, 1997; Christman *et al.*, 2002; Smith *et al.*, 2003). Sodium bentonite (Na-bentonite), where Na^+ is the predominant exchangeable cation, is used in nearly all of these applications. Na-bentonite is preferred to other types of bentonite, such as Ca-bentonite or Mg-bentonite, because Na-bentonite tends to swell to a greater extent in the presence of water leading to lower hydraulic conductivity, k, to water or dilute aqueous solutions containing inorganic or organic solutes (*i.e.* $k \leqslant 10^{-10}$ m/s) (*e.g.* Gleason *et al.*, 1997; Shackelford *et al.*, 2000). Also, Na-bentonite can exhibit substantial semipermeable membrane behavior for dilute concentrations of simple salts (Malusis *et al.*, 2001; Malusis and Shackelford, 2002a; Kang and Shackelford, 2009; Shackelford, 2011, 2012, 2013). Both membrane behavior and low k are beneficial in chemical containment applications, because: (1) low k results in limited advective (hydraulically driven) contaminant transport; and (2) membrane behavior promotes hyperfiltration, chemico-osmosis, and reduced diffusion of aqueous-phase chemicals (Shackelford *et al.*, 2003; Shackelford, 2011, 2012, 2013).

The aforementioned beneficial properties of bentonite, however, can be affected adversely by environmental conditions that promote exchange of multivalent cations for monovalent cations. Such cation exchange can cause collapse of the hydrated interlayer of the bentonite and limit osmotic swell, thereby potentially increasing the advective chemical mass flux and diffusion and decreasing hyperfiltration and chemico-osmotic counter flow (Malusis and Shackelford, 2002b; Manassero and Dominijanni, 2003; Kolstad *et al.*, 2004;

* E-mail address of corresponding author:
shackel@engr.colostate.edu
DOI: 10.1346/CCMN.2015.0630301

Shackelford and Sample-Lord, 2014). This incompatibility between chemicals in solution and Na-bentonite has spurred considerable interest in chemically modifying bentonites to be more compatible with the surrounding environment. For example, Na-bentonites have been amended with organic molecules for improved hydraulic and diffusive performance (*e.g.* Onikata *et al.*, 1996, 1999; Trauger and Darlington, 2000; Ashmawy *et al.*, 2002; Di Emidio, 2010; Di Emidio *et al.*, 2010; Mazzieri *et al.*, 2010a, 2010b; Di Emidio *et al.*, 2011; Mazzieri, 2011). In these cases, organic molecules were intercalated to increase the potential for osmotic swell in the presence of multivalent-for-monovalent cation exchange and/or elevated solute concentrations.

The bentonite investigated in the present study was modified chemically at the nanoscale with the intention of retaining the swollen structure of the bentonite. Organic molecules (acrylic acid) were inserted between the montmorillonite layers and then polymerized *in situ* to form an interconnected structure within the bentonite. Because this modification occurred at the nanoscale, the material has been referred to as a bentonite-polymer nanocomposite (BPN) (Scalia *et al.*, 2011; Scalia, 2012; Bohnhoff and Shackelford, 2013) or a bentonite-polymer composite (BPC) (Scalia *et al*., 2014). The BPC designation will be used herein.

The BPC evaluated here is different from other chemically treated or modified bentonites, such as organobentonites and the more typical anionic polymer modified bentonites. Organobentonites typically are synthesized either by solution or by solid-state reactions (Lagaly *et al.*, 2006). Also, anionic polymer-modified bentonites typically employ long-chain anionic polymers, such as the anionic polyacrylimides, that are electrostatically associated with the positively charged edges of the bentonite platelets (*e.g*. Boels and van der Wal, 1999; Heller and Keren, 2003). In contrast, the BPC evaluated here was formed by modifying Na-bentonite at the nanoscale by intercalation and *in situ* polymerization of acrylic acid, resulting in Na-polyacrylate both within and outside the interlayer regions (Scalia *et al.*, 2014).

Traditional Na-bentonites in the form of manufactured hydraulic barriers known as geosynthetic clay liners (GCLs) have been shown to exhibit semipermeable membrane behavior upon exposure to dilute solutions of KCl (*e.g.* Malusis and Shackelford, 2002a, 2002b; Kang and Shackelford, 2009, 2011). Similarly, the BPC evaluated here has also been shown to behave as a semipermeable membrane upon exposure to similar salt solutions (Bohnhoff and Shackelford, 2013). In the case of traditional Na-bentonites, the existence of such membrane behavior also has been shown experimentally to be correlated directly with solute diffusion through the Na-bentonite, whereby an increase in membrane efficiency toward that for an ideal (perfect) semipermeable membrane was shown to correlate with a decrease in the diffusive solute flux through Na-bentonite (Malusis and Shackelford, 2002b). This relationship also has been demonstrated theoretically by Dominijanni *et al.* (2013). A similar correlation between diffusion of salts and semipermeable membrane behavior has not been shown previously for the BPC evaluated in the present study, however. The primary question to be answered in this regard is whether or not the modification of the bentonite affects the salt-diffusion process. Because a decrease in diffusive solute flux is beneficial to the containment function of chemical containment barriers, the answer to this question is important from the viewpoint of the potential use of the BPC as an alternative to traditional bentonite in such chemical containment applications.

Accordingly, the purpose of this study was to evaluate the diffusive flux of a simple salt, *i.e.* KCl, through the BPC, and then correlate the diffusive properties with the previously measured membrane behavior of the BPC to ascertain if the BPC exhibited the same trend as previously observed for traditional Na-bentonite, *i.e.* decreasing diffusive salt flux with increasing semipermeable membrane behavior (*i.e*. solute restriction). Aside from representing what the authors believe to be the first evaluation of salt diffusion through a BPC reported in the literature, the study is unique in at least two other ways. First, unlike most previous studies where the specimens of Na-bentonite were flushed (leached) of soluble salts prior to testing to enhance the probability of significant semipermeable membrane behavior (*e.g.* Malusis and Shackelford, 2002a, 2002b), flushing of soluble salts was not performed on the specimens of the BPC evaluated here. Second, the previous study conducted by Malusis and Shackelford (2002b) for salt diffusion through the traditional Na-bentonite was based on the results of single-stage tests, whereas the salt-diffusion tests conducted for this study were multiple-stage tests.

MATERIALS AND METHODS

Materials

The BPC evaluated here was provided by Colloid Environmental Technologies Co. (CETCO, Hoffman Estates, Illinois, USA). The BPC was created using polyacrylic acid (PAA) and methods similar to those used in the production of polymer nanocomposites (*e.g.* Muzney *et al.*, 1996). In brief, Na-bentonite was added to a monomer solution to form a bentonite-monomer slurry. The monomer solution consisted of acrylic acid dissolved in water followed by neutralization with NaOH and the addition of an initiator, sodium persulfate. Polymerization was initiated by raising the temperature of the bentonite-monomer slurry above the decomposition temperature of the initiator molecule (180ºC), causing the initiator molecule to decompose into free radicals (R•). The R• reacted with the acrylic acid

https://doi.org/10.1346/CCMN.2015.0630301 Published online by Cambridge University Press

monomer to form more free radicals (RM•), which in turn reacted with additional monomer to proliferate the polymer chain (RMM•). The resulting polymer content of the BPC was reported to be 28.5% by mass (Scalia, 2012; Scalia *et al*., 2014).

The BPC was classified as a high-plasticity clay or CH according to the Unified Soil Classification System (ASTM D 2487). Mineralogical analyses conducted by Mineralogy, Inc. (Tulsa, Oklahoma, USA) using X-ray diffraction indicated the composition of the BPC as 76% montmorillonite, 15% quartz, 7% plagioclase feldspar, and 2% illite/mica.

Scalia (2012) and Scalia *et al.* (2014) report a measured cation exchange capacity, CEC, for the BPC of 142.6 meq/100 g, with sodium (Na^+) predominant in terms of both the bound cation composition (90% by mole fraction) and the soluble cation concentrations within the pore liquid (*i.e.* 118 meq/100 g Na^+, 9.5 meq/100 g Ca^{2+}, 1.6 meq/100 g Mg^{2+}, 0.4 meq/100 g K^+). In contrast, the CEC of the Na-bentonite used to produce the BPC was 85.5 meq/100 g. As with the BPC, sodium (Na^+) was predominant in terms of both the bound-cation composition (42% by mole fraction) and the soluble cation concentrations within the pore liquid (*i.e.* 23.3 meq/100 g Na^+, 0.2 meq/100 g Ca^{2+}, 0.1 meq/100 g Mg^{2+}, 0.4 meq/100 g K^+) for the Na-bentonite used to produce the BPC (Scalia, 2014). Additional details regarding the properties of the BPC can be found in Scalia *et al.* (2011, 2014), Bohnhoff (2012), Scalia (2012), and Bohnhoff and Shackelford (2013).

The liquids used in the present study included deionized water (DIW) (pH = 7.35, electrical conductivity, EC, at 25ºC = 0.06 mS/m) and solutions of DIW with potassium chloride (KCl) (certified A.C.S.; Fisher Scientific, Fair Lawn, New Jersey, USA) with measured concentrations ranging from 4.7 mM to 54 mM KCl. Concentrations of potassium (K^+) were measured using inductively coupled plasma-atomic emission spectrometry or ICP-AES (IRIS® Advantage/1000 ICAP Spectrometer, Thermo Jarrel Ash Co., Franklin, Massachusetts, USA), whereas concentrations of chloride (Cl^-) were measured using ion chromatography or IC (Dionex® 4000i IC Module, Dionex Co., Sunnyvale, California, USA). The measured pH of the KCl solutions ranged from 5.20 to 5.31 and the measured EC at 25ºC ranged from 70.7 to 661 mS/m.

Testing apparatus and procedures

The testing apparatus and procedures used in this study were similar to those described in detail by Malusis *et al.* (2001) and Kang and Shackelford (2009). In general, a water-saturated specimen of the BPC was confined in either a rigid-wall cell or a flexible-wall cell. A solution with an initial concentration of KCl, C_{ot} (> 0), was circulated through a porous disk along the top of the specimen while DIW (C_{ob} = 0) was circulated simultaneously through a porous disk along the base of the specimen. The system was closed during membrane testing, such that no liquid flow was allowed through the specimen in order to maintain a constant volume. As a result, a pressure built up on the high-concentration side (*i.e.* top) of the specimen during circulation of KCl to counteract the tendency for chemico-osmotic liquid flow from the bottom to the top of the specimen (*i.e.* from low concentration to high concentration). The pressures in the top and bottom circulation lines were measured continuously using in-line pressure transducers, and the difference in pressure across the specimen, ΔP, which represented the chemico-osmotic pressure, was monitored directly using a differential pressure transducer. The ratio of the measured ΔP and the maximum chemico-osmotic pressure difference, $\Delta\pi$, based on the difference in boundary salt concentrations, equates to the magnitude of the chemico-osmotic efficiency coefficient, ω (= $\Delta P/\Delta\pi$), which varies from zero for no solute restriction (*i.e.* no membrane behavior) to unity for complete solute restriction (ideal membrane behavior).

For specimens that are not ideal membranes (*i.e.* $\omega < 1$), solutes diffuse from the top to the bottom of the specimen (*i.e.* from high concentration to low concentration). In the present case, diffusion resulted in Cl^- and K^+ concentrations in the outflow from the specimen base, C_b, that were greater than those in the inflow to the specimen base ($C_b > C_{ob}$), whereas Cl^- and K^+ concentrations in the outflow from the specimen top, C_t, were lower than those in the inflow at the specimen top ($C_t < C_{ot}$). As a result, the Cl^- and K^+ concentrations in the outflows from the specimen bottoms (*i.e.* C_b) were monitored as a function of time to determine the diffusive solute mass flux required to determine the diffusion coefficients.

Measurement of diffusion coefficients

As long as the concentration boundaries are maintained reasonably constant, solute diffusion through a specimen will eventually reach a steady-state diffusive mass flux. This method of measuring effective diffusion coefficients is commonly referred to as the steady-state, time-lag, or through-diffusion method (*e.g.* Shackelford, 1991; Shackelford and Moore, 2013). Details of this method are provided elsewhere (*e.g.* Shackelford, 1991; Shackelford and Lee, 2003). In brief, the concentrations of solutes that have diffused through the specimen (Cl^- and K^+ in this study) are converted to the area-normalized cumulative mass (Q_t), or

$$Q_t = \frac{1}{A}\sum_{i=1}^{N_s} \Delta m_i = \frac{1}{A}\sum_{i=1}^{N_s} C_{b,i}\Delta V_i \qquad (1)$$

where A is the cross-sectional area of the specimen, Δm_i is the incremental mass of the solute species collected over a time increment, Δt, $C_{b,i}$ is the mass concentration of the solute species in the incremental volume, ΔV_i, of the circulation outflow from the bottom boundary of the

https://doi.org/10.1346/CCMN.2015.0630301 Published online by Cambridge University Press

specimen, corresponding to Δt, and i is an integer index in the summation series that designates each collected sample, which varies from 1 to the total number of incremental samples, N_s, corresponding to the total elapsed time, t. An important constraint in the use of equation 1 is that all solute mass must be included, such that sampling must be continuous, although the magnitude of ΔV_i can vary. The data are typically plotted as Q_t *vs.* the cumulative elapsed time, t. The plot is generally non-linear at the beginning or transient stage of the test, which is followed by a steady-state stage indicated by a straight line representing constant diffusive solute mass flux (Shackelford, 1991; Shackelford and Lee, 2003; Shackelford and Moore, 2013).

In the present study, values of the effective diffusion coefficient, D^*, were determined in two ways, *i.e.* by performing a linear regression of only the steady-state portion of the data, and by performing a non-linear regression of all of the data. Differences between the two determined D^* values reflect, in part, the influence of solute–solute interactions that can occur during the transient stage of the test due to the presence of other ionic species initially within the porewater of the specimens (Shackelford, 1991; Shackelford and Daniel, 1991).

The following expression was used to determine D^* by linear regression of the steady-state portion of the Q_t *vs.* t data (Shackelford, 1991):

$$D^* = -\left(\frac{\Delta Q_t}{\Delta t}\right)\left(\frac{L}{n w_A \Delta C}\right) \quad (2)$$

where $\Delta Q_t/\Delta t$ represents the slope of the linear regression, L is the specimen thickness, n is the specimen porosity, w_A is the atomic weight of the diffusing solute, and ΔC<O is the molar concentration difference of the solute (*i.e.* Cl^- or K^+). In applying equation 2, a sequential linear regression as described by Shackelford and Lee (2003) was conducted on the measured data to establish the number of measured data representing the steady-state diffusive mass flux. Briefly, a linear regression was conducted on an increasing number of Q_t-*vs.*-t data until the coefficient of determination, r^2, deviated significantly from unity, corresponding to the distinction between the transient and steady-state portions of the data or the time to steady state.

The non-linear regression analysis was performed by fitting the following solution to Fick's second law for the case of diffusion through porous media with a constant inlet concentration C_1 at $x = 0$ and outlet concentration C_2 ($C_2 << C_1$) at $x = L$ (*e.g.* Crank, 1975; Skagius and Neretnieks, 1986) to the complete set of data (*i.e.* both the transient and the steady-state data):

$$Q_t = LC_1\left[\frac{D^* n t}{L^2} - \frac{R_d n}{6} - \frac{2R_d n}{\pi^2}\sum_{i=1}^{\infty}\frac{(-1)^i}{i^2}\exp\left(-\frac{D^* n i^2 \pi^2 t}{L^2 R_d n}\right)\right] \quad (3)$$

where R_d ($\geqslant 1$) is the retardation factor of the solute which takes into account the possibility of linear, reversible, and instantaneous sorption, and i is an integer index in the summation series which varies from 1 to infinity. Equation 3 was fitted to the measured data by non-linear regression using *Mathcad* (2007, Parametric Technology Corporation, Needham, Massachusetts, USA) to determine simultaneously both D^* and R_d.

The parameter D^* determined using either equation 2 or 3 for each solute species (*i.e.* Cl^- or K^+) is defined as follows (Shackelford and Daniel, 1991):

$$D^* = D_o \tau_a \quad (4)$$

where D_o is the aqueous-phase or free-solution diffusion coefficient of the solute, and τ_a is an apparent tortuosity factor ($0 \leqslant \tau_a \leqslant 1$) representing the product of the actual matrix (geometric) tortuosity factor, τ_m, and a restrictive tortuosity factor, τ_r, or (Malusis and Shackelford, 2002b; Shackelford and Moore, 2013):

$$\tau_a = \tau_m \tau_r = \tau_m \prod_{i=1}^{N} \tau_i = \tau_m(\tau_1 \tau_2 \cdots \tau_N) \quad (5)$$

where τ_r represents the product of N other factors (τ_i) that contribute to the apparent tortuosity factor by acting to reduce or restrict the diffusive solute mass flux through the porous medium, such as anion exclusion, increased water viscosity near the surface of clay particles, *etc*., and i is an integer index in the product series that varies from 1 to N.

Testing program

Multiple-stage membrane/diffusion tests were conducted in this study by sequentially circulating four KCl solutions with increasingly higher source concentrations, C_{ot}, of 4.7, 9.3, 20, and 54 mM KCl across the top boundary of the specimen for each test, while simultaneously circulating DIW across the bottom boundary of the specimen (*i.e.* $C_{ob} = 0$). As a result, the slope of Q_t *vs.* t increased with increasing concentration of KCl; *i.e.* a greater diffusive solute mass flux occurred as a result of the greater concentration gradient imposed across the specimen. Thus, net values of Q_t and t, or Q_t' and t', respectively, pertaining to each individual stage (*i.e.* C_{ot}) of the test, were used to evaluate D^* for each solute. The use of Q_t' and t' for each stage of the test essentially amounts to resetting Q_t and t to zero for the evaluation of D^* for each subsequent stage of the test. The criterion used to determine the duration of each stage was a sufficient number of data to provide a high value for the coefficient of determination, r^2 (> 0.995), with respect to linear regression of the straight-line or steady-state portion of the data for K^+.

Four multiple-stage tests were conducted, two using a rigid-wall (RW) cell and two using a flexible-wall (FW) cell. The rigid-wall tests, designated as RW1 and RW2, corresponded to specimen thicknesses, L, of 16.7 mm and 8.6 mm and total specimen porosities, n, of 0.92 and 0.80, respectively. The flexible-wall tests, designated as

https://doi.org/10.1346/CCMN.2015.0630301 Published online by Cambridge University Press

FW1 and FW2, corresponded to initial effective stresses, σ', of 34.5 kPa and 103 kPa, respectively, and initial values of n immediately after consolidation, but prior to membrane testing, of 0.95 and 0.84, respectively. As previously noted, the circulation outflow from the bottom of the specimens was analyzed for concentrations, C_b, of Cl^- (IC) and K^+ (ICP), and the concentrations were then used to determine D^*. The membrane efficiency coefficient, ω, was measured simultaneously using the procedures described by Malusis *et al.* (2001) and Kang and Shackelford (2009), and the results of these measurements were reported by Bohnhoff (2012) and by Bohnhoff and Shackelford (2013).

RESULTS AND DISCUSSION

Bottom outflow concentrations

The measured concentrations of anions (*i.e.* Cl^-, F^-, and SO_4^{2-}) and cations (Ca^{2+}, K^+, and Na^+) in the circulation outflows from the bottom of the cell (C_b) are a function of each testing stage (*i.e.* C_{ot} = 4.7, 9.3, 20, and 54 mM KCl) for each test (Figure 1). The predominant chemical species in the circulation outflows for all tests were Cl^-, K^+, and Na^+, whereas the values of C_b for F^-, SO_4^{2-}, and Ca^{2+} were low (*i.e.* near the detection limit) and relatively negligible throughout all tests.

For each test, C_b of both Cl^- and K^+ increased with each subsequent stage of each test as expected on the basis of the increase in the source concentration, C_{ot}, of KCl. The concentrations of Na^+ measured in the bottom circulation outflow of the cell represent the excess Na^+ initially present within the BPC (Scalia, 2012). Also, the concentrations of Na^+ exiting the bottom of the cell exceeded the concentrations of K^+ during the first two stages (*i.e.* C_{ot} = 4.7 mM and 9.3 mM KCl) for all four tests (refer to Figure 1). However, during the last stage of the tests, when 54 mM KCl (= C_{ot}) was being circulated across the top of the specimens, the concentrations of K^+ in the bottom of the cell exceeded the concentrations of Na^+, due to increased diffusion of K^+ through the BPC and a continually diminishing amount of remnant Na^+ within the pore water of the BPC. Finally, the concentrations of Cl^- reached steady state more quickly than those of K^+, primarily due to exchange of K^+ for Na^+ and the electroneutrality constraint resulting primarily from the excess Na^+ initially present within the porewater of the BPC.

Diffusion results

The slopes, $\Delta Q_t'/\Delta t'$, resulting from linear regressions of the steady-state portions of individual plots of $Q_{t'}$ *vs.* t' for each solute (*i.e.* Cl^- and K^+) ranged from 48.4 to 2020 mg/m^2-d for Cl^- and from 2.37 to 1600 mg/m^2-d for K^+ (Figures 2–5 for tests RW1, RW2, FW1, and FW2, respectively). Values of $\Delta Q_t'/\Delta t'$ increased with increasing C_{ot}, as expected, due to a greater diffusive solute mass flux with increasing concentration gradient. The lower magnitudes in $\Delta Q_t'/\Delta t'$ for K^+ resulted from the existence of remnant Na^+ initially present in the pore liquid of the BPN specimens (*i.e.* because the specimens were not flushed of remnant ions prior to testing), which contributed to the positive charge required for electroneutrality during diffusion.

The D^* values based on the linear regression of the steady-state portion of the data for each stage of each test are designated as D^*_{ss}, and those resulting from the non-linear regression of the full data set for each stage of each test are designated as D^*_{nl} (Table 1). In terms of the effect of C_{ot} on the measured values of D^*, three observations are readily apparent (Figure 6).

First, the values of D^*_{ss} were slightly higher than the values of D^*_{nl}, with the differences in values being most evident at the lowest C_{ot} of 4.7 mM KCl (Figure 6). The ratio of the D^*_{ss} to the D^*_{nl} (*i.e.* D^*_{ss}/D^*_{nl}) varied from 0.84 to 1.54, with most values of D^*_{ss}/D^*_{nl} (> 62.5%) within the narrow range of 1.02 to 1.09. Thus, the values of D^*_{ss} and D^*_{nl} were generally similar, with the values of D^*_{ss} being consistently, albeit only slightly, higher than the values of D^*_{nl}. The slight differences in the values of D^*_{ss} relative to those of D^*_{nl} can be attributed, in part, to the aforementioned initial dominance of Na^+ relative to K^+ in the porewater of the BPC (see Figure 1) and the similarity in the diffusive mobilities of NaCl and KCl as reflected by their respective D_o values of 1.610×10^{-9} m^2/s and 1.993×10^{-9} m^2/s (Shackelford and Daniel, 1991).

Second, the values of D^* (either D^*_{ss} or D^*_{nl}) for either Cl^- or K^+ tended to increase with increasing C_{ot} of KCl. As indicated by the values of ω and C_{ot} in Table 1, ω decreased with increasing C_{ot}, which is consistent with the results of previous studies (*e.g.* see Malusis and Shackelford, 2002a; Shackelford *et al.*, 2003; Shackelford, 2011, 2012, 2013). This decrease in ω with increasing C_{ot} resulted in greater solute mass flux, such that the increase in D^* with increasing C_{ot} can be attributed to a decrease in solute restriction (*i.e.* τ_r) with increasing C_{ot}.

Third, at a given C_{ot}, the values of D^* for K^+ were generally lower than those for the Cl^-, with differences between the respective values of D^* decreasing with increasing C_{ot}. For example, for test FW1, D^*_{ss,Cl^-} was 1.7×10^{-10} and D^*_{ss,K^+} was 4.3×10^{-12} m^2/s during circulation of 4.7 mM KCl, whereas D^*_{ss,Cl^-} was 2.9×10^{-10} m^2/s and the D^*_{ss,K^+} was 2.0×10^{-10} m^2/s during circulation with 54 mM KCl.

These same results can be viewed more conveniently in terms of values of the ratio, $D^*_{ss,Cl^-}/D^*_{ss,K^+}$ (Figure 7). For example, values of $D^*_{ss,Cl^-}/D^*_{ss,K^+}$ were highest at a C_{ot} of 4.7 mM KCl (*e.g.* 36.9 for test RW1), and decreased toward unity with increasing C_{ot} (*e.g.* $D^*_{ss,Cl^-}/D^*_{ss,K^+}$ is 1.08 for test RW2 with C_{ot} of 54 mM). These differences between D^*_{ss,Cl^-} and D^*_{ss,K^+}, especially at the lower values of C_{ot}, which ostensibly violate the

https://doi.org/10.1346/CCMN.2015.0630301 Published online by Cambridge University Press

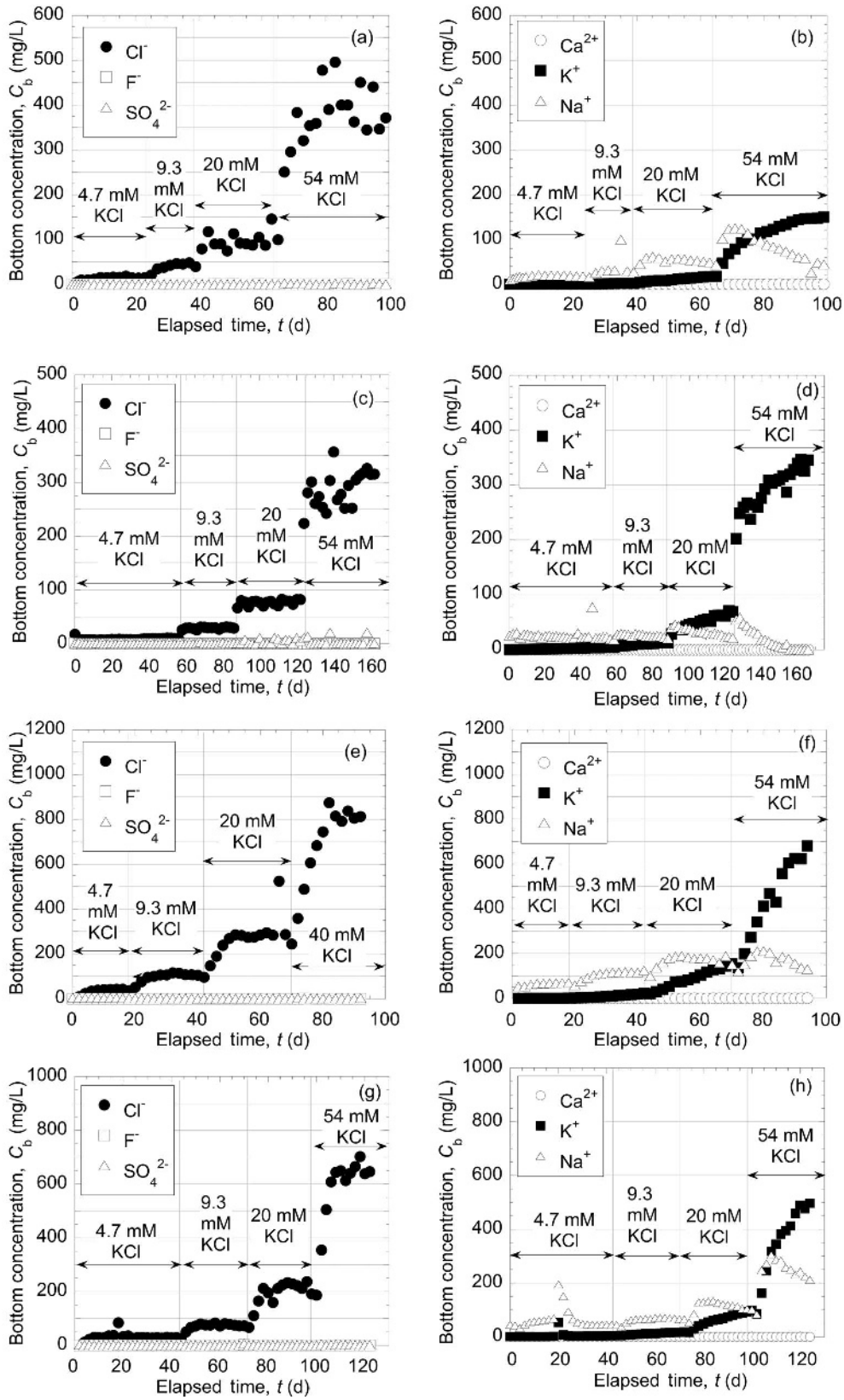

Figure 1. Measured concentrations of anions and cations in the circulation outflow from the bottom of the specimen for each test: (a, b) RW1; (c, d) RW2; (e, f) FW1; and (g, h) FW2.

https://doi.org/10.1346/CCMN.2015.0630301 Published online by Cambridge University Press

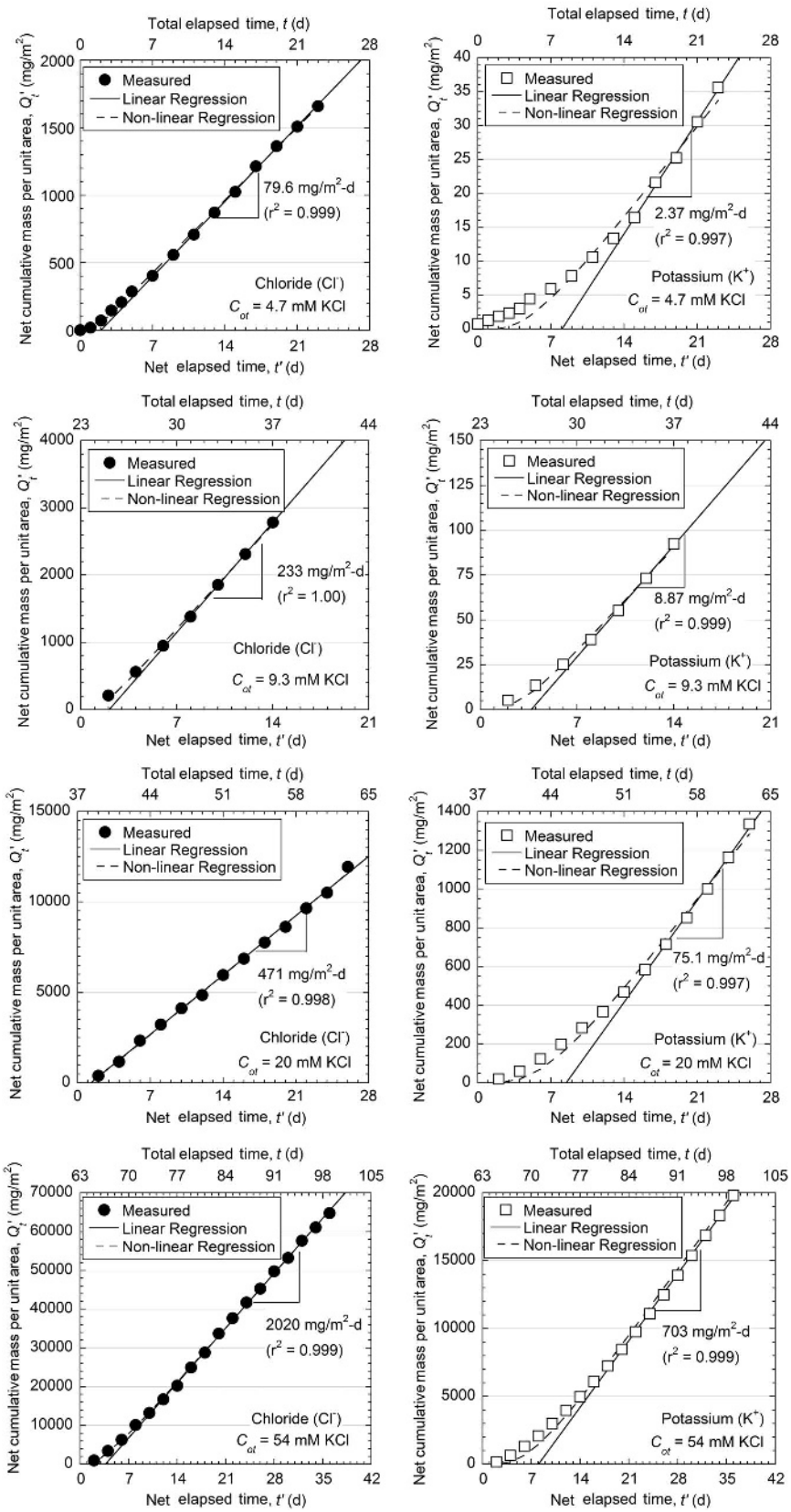

Figure 2. Diffusion test results for test RW1 (porosity, $n = 0.92$).

https://doi.org/10.1346/CCMN.2015.0630301 Published online by Cambridge University Press

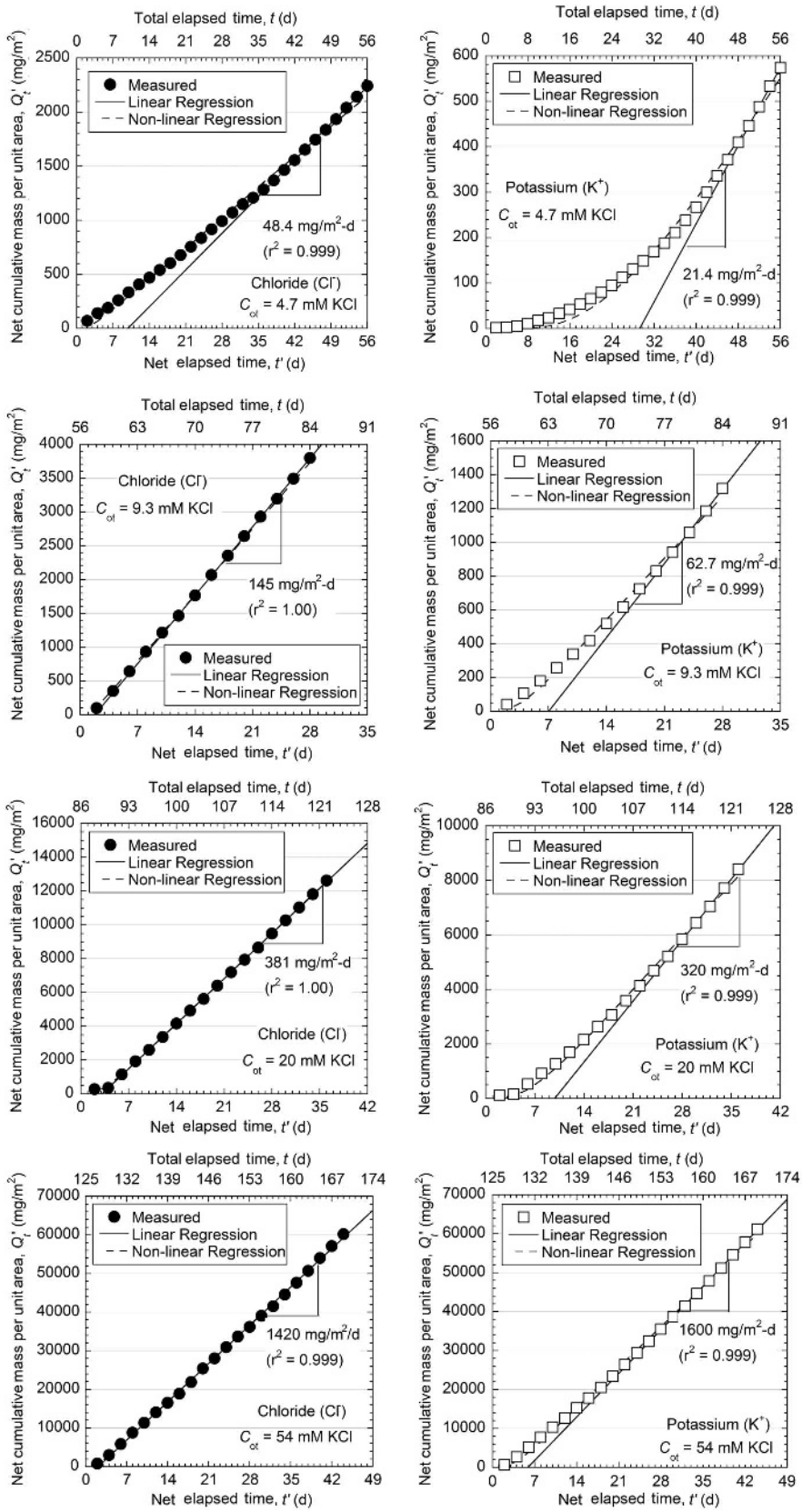

Figure 3. Diffusion test results for test RW2 (porosity, $n = 0.80$).

https://doi.org/10.1346/CCMN.2015.0630301 Published online by Cambridge University Press

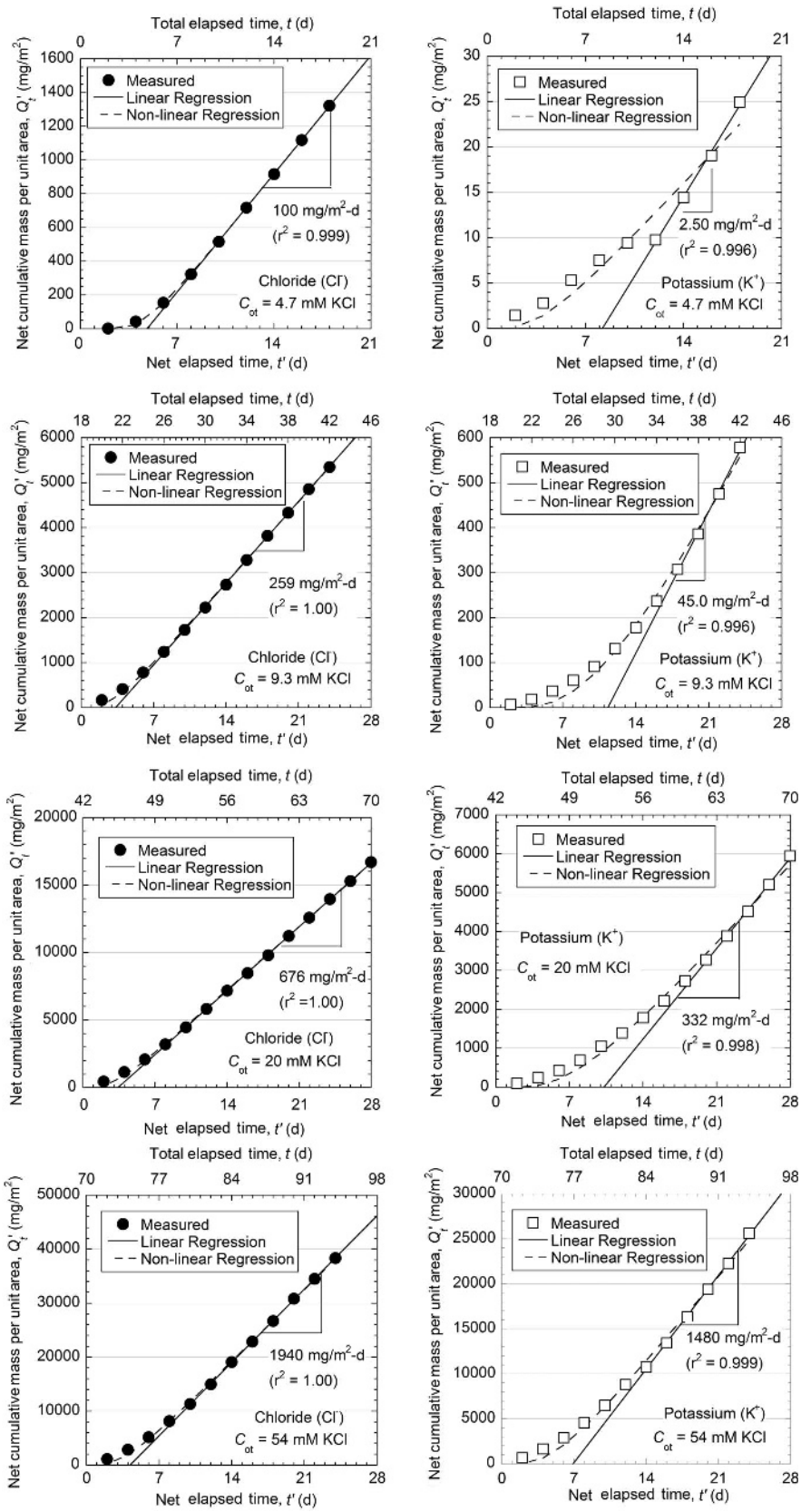

Figure 4. Diffusion test results for test FW1 (effective stress, $\sigma' = 34.5$ kPa).

https://doi.org/10.1346/CCMN.2015.0630301 Published online by Cambridge University Press

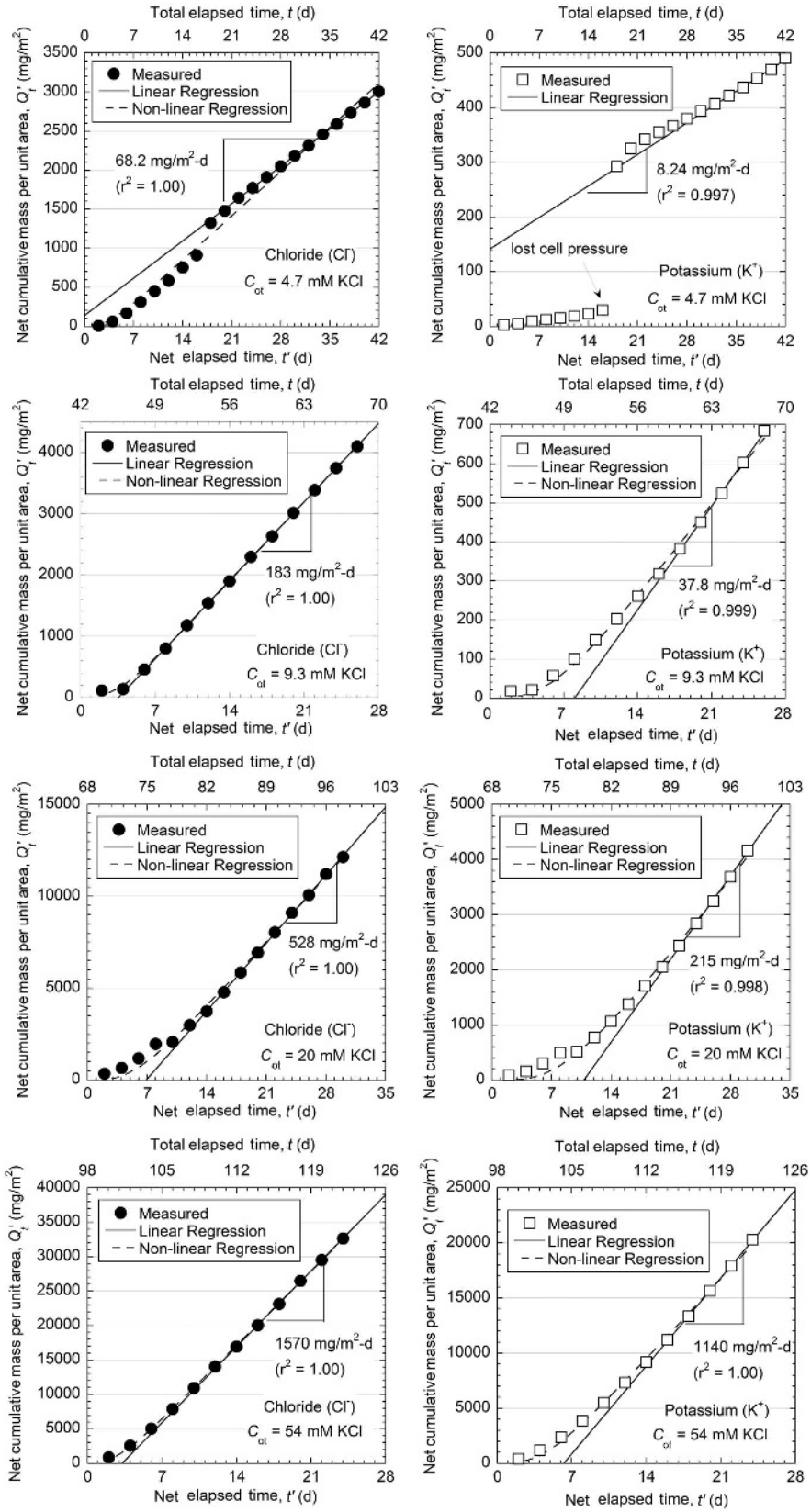

Figure 5. Diffusion test results for test FW2 (effective stress, $\sigma' = 103$ kPa).

https://doi.org/10.1346/CCMN.2015.0630301 Published online by Cambridge University Press

Table 1. Results of membrane testing and diffusion analysis for bentonite-polymer composite (BPC) using rigid-wall (RW) and flexible-wall (FW) cells.

Test	Porosity, n	Initial effective stress, σ' (kPa)	Source KCl concentration, C_{ot} (mM)	Membrane efficiency coefficient, ω[(a)]	Solute	Effective diffusion coefficient, D^* (m^2/s) Linear[(b)]	Non-linear[(c)]
RW1	0.92	NA	4.7	0.80	Cl^-	1.0×10^{-10}	9.7×10^{-11}
					K^+	2.7×10^{-12}	2.2×10^{-12}
			9.3	0.65	Cl^-	1.5×10^{-10}	1.4×10^{-10}
					K^+	5.1×10^{-12}	4.8×10^{-12}
			20	0.43	Cl^-	1.4×10^{-10}	1.4×10^{-10}
					K^+	2.0×10^{-11}	1.8×10^{-11}
			54	0.17	Cl^-	2.2×10^{-10}	2.2×10^{-10}
					K^+	7.0×10^{-11}	6.6×10^{-11}
RW2	0.80	NA	4.7	0.88	Cl^-	3.7×10^{-11}	3.0×10^{-11}
					K^+	1.5×10^{-11}	1.3×10^{-11}
			9.3	0.73	Cl^-	5.5×10^{-11}	5.5×10^{-11}
					K^+	2.2×10^{-11}	1.8×10^{-11}
			20	0.46	Cl^-	6.8×10^{-11}	6.8×10^{-11}
					K^+	5.1×10^{-11}	4.5×10^{-11}
			54	0.20	Cl^-	1.0×10^{-10}	9.3×10^{-11}
					K^+	9.5×10^{-11}	8.9×10^{-11}
FW1	0.94 −0.95	34.5	4.7	0.55	Cl^-	1.7×10^{-10}	1.7×10^{-10}
					K^+	4.3×10^{-12}	2.8×10^{-12}
			9.3	0.32	Cl^-	2.2×10^{-10}	2.2×10^{-10}
					K^+	3.5×10^{-11}	3.5×10^{-11}
			20	0.14	Cl^-	2.7×10^{-10}	2.7×10^{-10}
					K^+	1.2×10^{-10}	1.1×10^{-10}
			54	0.04	Cl^-	2.9×10^{-10}	2.8×10^{-10}
					K^+	2.0×10^{-10}	1.8×10^{-10}
FW2	0.78 −0.84	103	4.7	0.46	Cl^-	7.3×10^{-11}	8.7×10^{-11}
					K^+	8.0×10^{-12}	−−
			9.3	0.38	Cl^-	9.9×10^{-11}	1.0×10^{-10}
					K^+	1.9×10^{-11}	1.7×10^{-11}
			20	0.25	Cl^-	1.4×10^{-10}	1.3×10^{-10}
					K^+	5.1×10^{-11}	4.7×10^{-11}
			54	0.10	Cl^-	1.6×10^{-10}	1.5×10^{-10}
					K^+	1.0×10^{-10}	9.5×10^{-11}

[(a)] Steady-state membrane efficiency coefficient based on initial (source) salt concentrations as reported by Bohnhoff and Shackelford (2013).
[(b)] Based on linear regression of the apparent steady-state data only.
[(c)] Based on non-linear regression of all of the data.

requirement for electroneutrality, can be attributed to the confounding influence of the significant concentration of remnant Na^+ initially in the pore liquid of the BPC specimens and the exchange of K^+ primarily for initially bound Na^+ (see subsequent discussion on electroneutrality and cation exchange).

In addition, the values of $D^*_{ss,Cl^-}/D^*_{ss,K^+}$ for tests RW2 and FW2 were lower than those for tests RW1 and FW1. The lower values of $D^*_{ss,Cl^-}/D^*_{ss,K^+}$ for tests RW2 and FW2 compared to tests RW1 and FW1 can be attributed to a lower porosity ($n = 0.80$ *vs.* $n = 0.92$ for tests RW2 and RW1, respectively) or the greater effective stress ($\sigma' = 103$ kPa *vs.* 34.5 kPa for tests FW2 and FW1, respectively), which resulted in lower values of D^*_{ss,Cl^-} especially at lower values of C_{ot}. For example, during the circulation of 4.7 mM KCl, the D^*_{ss,Cl^-} for test RW1 was 1.0×10^{-10} m^2/s, whereas D^*_{ss,Cl^-} for test RW2 was 3.7×10^{-11} m^2/s. The values of $D^*_{ss,Cl^-}/D^*_{ss,K^+}$ for test FW2 also may be lower than those for test FW1 as a result of drainage that occurred during consolidation of the specimen in test FW2 to a greater effective stress (*i.e.* $\sigma' = 103$ kPa), as such drainage tends to reduce the amount of soluble cations, primarily Na^+, initially in the pore liquid of the specimen (see subsequent discussion on electroneutrality and cation exchange).

Consideration of electroneutrality and cation exchange

The aforementioned difference between D^*_{ss,Cl^-} and D^*_{ss,K^+} in this study for the BPC is in contrast to previous results reported by Malusis and Shackelford (2002b) that

https://doi.org/10.1346/CCMN.2015.0630301 Published online by Cambridge University Press

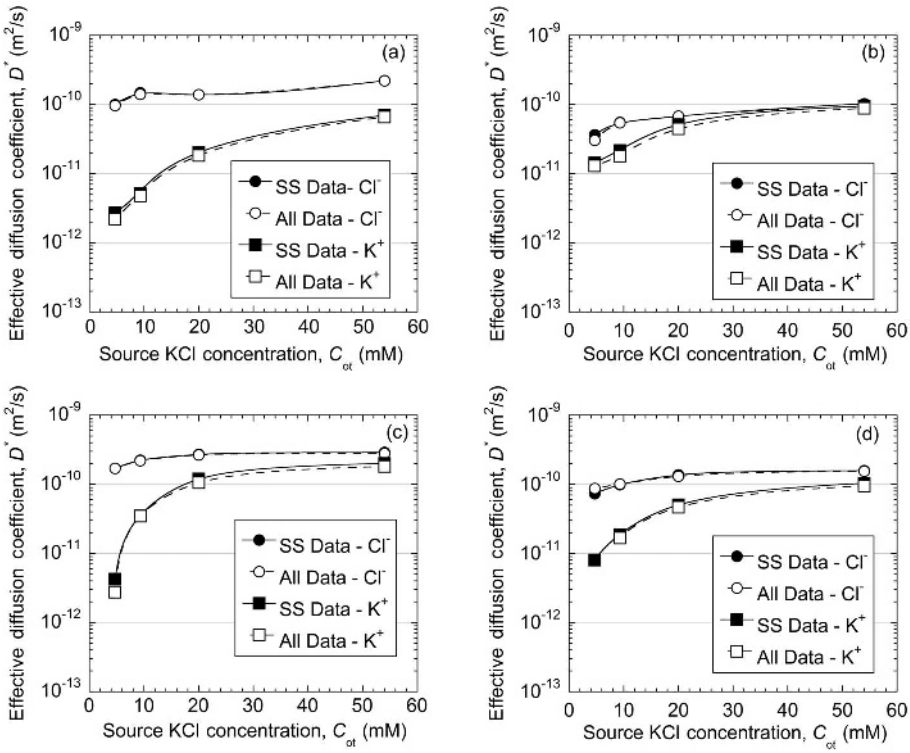

Figure 6. Effective diffusion coefficients of chloride (Cl^-) and potassium (K^+) *vs.* source KCl concentration for diffusion through bentonite-polymer composite (BPC) based on linear regression of steady-state (SS) data and non-linear regression of all data from rigid-wall (RW) and flexible-wall (FW) tests: (a) RW1; (b) RW2;(c) FW1; (d) FW2.

essentially show equivalency between D^*_{ss,Cl^-} and D^*_{ss,K^+} for diffusion through specimens containing conventional Na-bentonite. The difference in results can be attributed to the difference in the specimen-preparation procedures for the two studies. Specifically, unlike the study by Malusis and Shackelford (2002b), the BPC specimens in this study were not flushed (leached) of remnant soluble salts existing within the pore liquid of the BPC specimens prior to testing. The existence of these remnant soluble salts, predominantly Na^+, in the BPC prior to testing (see Figure 1) can result in significant differences between D^*_{ss,Cl^-} and D^*_{ss,K^+}.

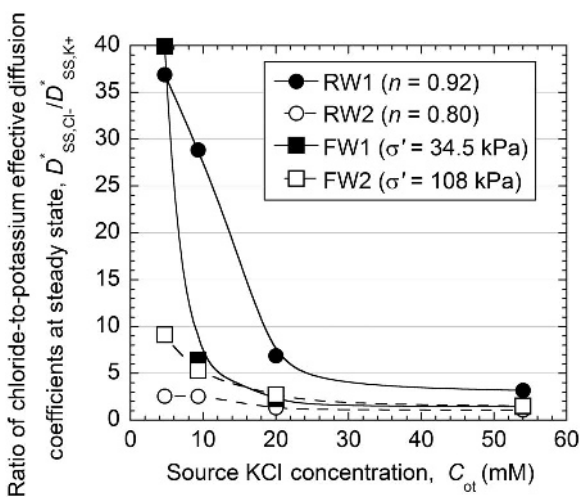

Figure 7. Ratio of chloride-to-potassium effective diffusion coefficients at steady state *vs.* source KCl concentration for specimens of bentonite-polymer composite (BPC) for both rigid-wall (RW) and flexible-wall (FW) tests [n = specimen porosity; σ' = initial effective stress in specimen].

For example, electroneutrality requires charge flux balance between the anions and the cations diffusing through the system (*e.g.* Shackelford and Lee, 2003). For the current study involving primarily Cl^-, K^+, and Na^+, this requirement can be written as follows:

$$J_{d,Cl^-}(-z_{Cl^-}) = J_{d,K^+}(z_{K^+}) + J_{d,Na^+}(z_{Na^+}) \quad (6)$$

where J_d represents the diffusive molar flux of the noted ionic species (*i.e.* Cl^-, K^+, and Na^+) and z represents the charges of Cl^-, K^+, and Na^+ (-1, $+1$, and $+1$, respectively). The J_d for the different ionic species can be written following Fick's first law for diffusion in soil as follows (*e.g.* Shackelford and Daniel, 1991):

$$J_d = nD^* i_c \quad (7)$$

where i_c is the molar concentration gradient of each ionic species. Because n should be constant for a given specimen and a given stage of testing, substitution of equation 7 into equation 6 for each ionic species results in the following expression:

$$D^*_{Cl^-}(i_{c,Cl^-}) = D^*_{K^+}(i_{c,K^+}) + D^*_{Na^+}(i_{c,Na^+}) \quad (8)$$

https://doi.org/10.1346/CCMN.2015.0630301 Published online by Cambridge University Press

As noted previously, the diffusion tests in this study were conducted by circulating solutions of KCl across the top of the specimen and DIW along the base of the specimen (Figure 8a). Therefore, at steady-state diffusive molar flux, the concentration gradients for Cl^- and K^+ across the specimen should be equivalent, or $i_{c,Cl^-} = i_{c,K^+} = i_c$. However, the value of i_{c,Na^+}, which resulted from the existence of excess Na^+ within the BPC prior to testing, varied as a function of time and location within the specimen due to diffusion of Na^+ from within the specimen to both the top and bottom boundaries of the specimen during testing (Figure 8b). Based on these considerations, equation 8 can be reduced to the following expression:

$$D^*_{Cl^-} = D^*_{K^+} + D^*_{Na^+}(I_c) \quad (9)$$

where I_c is the ratio of i_{c,Na^+} to i_c. Thus, in accordance with equation 9, the equivalency between $D^*_{Cl^-}$ and $D^*_{K^+}$ will depend on the value of I_c. That is, for values of $I_c > 0$, $D^*_{Cl^-} > D^*_{K^+}$, whereas $D^*_{K^+}$ approaches $D^*_{Cl^-}$ in the limit as I_c approaches zero (*i.e.* $D^*_{K^+} \rightarrow D^*_{Cl^-}$ as $I_c \rightarrow 0$).

As inferred from the measured concentrations of Cl^-, K^+, and Na^+ in the circulation outflows from the bottom of the test specimens (Figure 1), the value of i_{c,Na^+} was probably significantly greater than the value of i_c during the earlier stages of each test corresponding to circulation of the relatively dilute solutions of KCl (*i.e.* 4.7 and 9.3 mM). As a result, the value of I_c in equation 9 was probably significantly greater than zero, resulting in the values of $D^*_{K^+}$ being significantly lower than the values of $D^*_{Cl^-}$ in accordance with equation 9 (Figures 5, 6). The amount of Na^+ remaining in the specimens diminished with time, however (*i.e.* $i_{c,Na^+}\downarrow$ as $t\uparrow$), and the source concentrations of KCl used in the tests increased with time ($i_c\uparrow$ as $t\uparrow$), such that the value of I_c decreased toward zero with increasing duration of each test (*i.e.* $I_c \rightarrow 0$ as $t\uparrow$) (Figure 8b). Thus, in accordance with equation 9, the measured values of $D^*_{K^+}$ increased and approached those of $D^*_{Cl^-}$, which increased only slightly throughout the tests as the source concentration of KCl increased, *i.e.* due to the aforementioned effect of decreasing ω and increasing D^* with increasing C_{ot}. A more rigorous solution for the assessment of the equivalent effective diffusion coefficient in the case of electrolyte solutions has recently been proposed by Dominijanni and Manassero (2012a, 2012b), but consideration of this solution was beyond the scope of the present study.

Another complicating factor not considered in Figure 8 is the effect of cation exchange resulting from replacement of initially bound Na^+ with K^+ during diffusion of K^+ through the specimens. Such exchange is clearly evident from the differences in the values of the time lag, t_L' (*i.e.* the *x*-axis intercepts in the data shown in Figures 2–5), where the values of t_L' for K^+ are greater than those for Cl^- in all stages of all tests except for the first stage of test FW2 (see Figure 5). For the case where Cl^- and K^+ are the only diffusing ions, the diffusive molar fluxes (moles/m^2-d) of both Cl^- and K^+ must be equal at steady state due to the requirement for charge balance, *i.e.* as both of these ionic species are monovalent (*e.g.* see Shackelford and Lee, 2003). In this case, the diffusive mass flux (mg/m^2-d) for K^+ at steady state must be a factor of 1.10 greater than that for Cl^- at true steady state, as the atomic weight for K^+ is 1.10 times greater than that for Cl^- (*i.e.* 39.0983/35.453 ≈ 1.10). However, based on the diffusive mass fluxes at steady state shown in Figures 2–5 , this requirement was only achieved for the last stage (C_{ot} = 54 mM KCl) of test RW2 (Figure 9). Thus, even though the values of the coefficient of determination, r^2, for the linear regressions of the steady state portions of the data in Figures 2–5 were all close to unity ($r^2 \geqslant 0.996$), suggesting that steady-state conditions had been reached, the K^+ data clearly were not at steady state due to cation exchange.

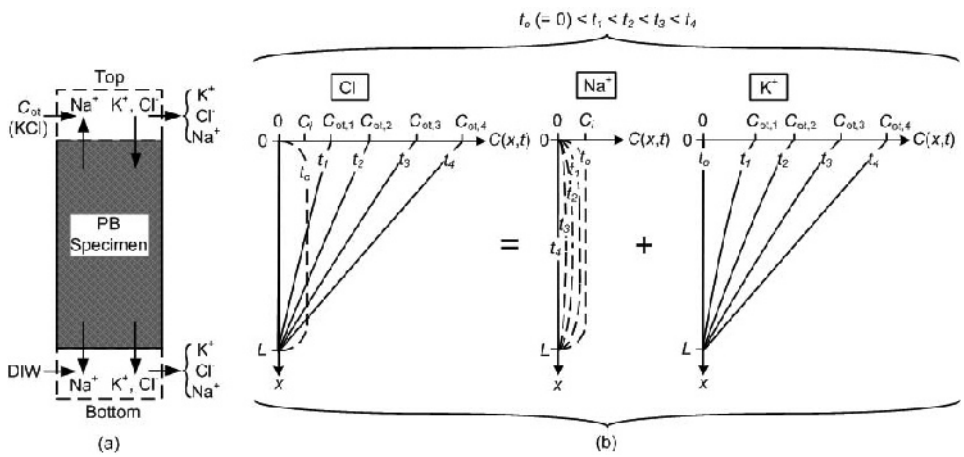

Figure 8. Conceptual illustration of concentration profiles of dominant ionic species in unflushed test specimens of bentonite-polymer composite (BPC) during diffusion testing: (a) directions of diffusion at top and bottom boundaries; (b) time-dependent concentration profiles.

https://doi.org/10.1346/CCMN.2015.0630301 Published online by Cambridge University Press

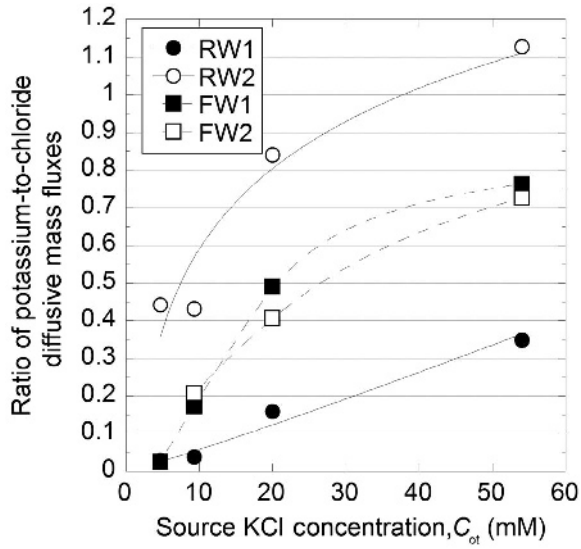

Figure 9. Ratio of potassium-to-chloride diffusive mass fluxes as a function of the source KCl concentration circulated through the top of the specimen.

In fact, equilibrium replacement of Na^+ with K^+ for any given stage of a test would probably have required extended periods that were well beyond those employed in the tests conducted in the present study. For example, Jo *et al.* (2005) permeated GCLs containing Na-bentonite with solutions containing from 5 mM to 20 mM $CaCl_2$, and found that the times required for complete replacement of exchangeable Na^+ by Ca^{2+}, whereby the measured concentrations of Na^+ in the effluent were below the detection limit (0.2 mg/L), ranged from 1.49 to 1.93 y. Thus, in spite of the large r^2 values associated with the values of D^*_{ss,K^+}, K^+ had probably not actually reached steady-state diffusion due to continual exchange of K^+ for Na^+ initially dominating the exchange sites of the BPC.

Correlation between diffusion and membrane behavior

The values of D^*_{ss,Cl^-} can be correlated with the associated values of ω (Table 1). The values of D^*_{ss,Cl^-} decreased with increasing ω as expected (Figure 10a), because solute transport becomes increasingly more restricted as the membrane behavior trends toward that of a perfect membrane (*i.e.* ω → 1) (Malusis and Shackelford, 2002b).

In general, the apparent tortuosity factor, τ_a, representing the effect of the porous media on the rate of solute diffusion, varies from zero when there are no interconnected pores corresponding to a perfect or ideal semipermeable membrane to unity when there is no porous medium (Shackelford and Daniel, 1991). That is, an increase in the value of τ_a reflects a less tortuous pathway and/or less solute restriction by membrane behavior (Malusis and Shackelford, 2002b). Accordingly, values of τ_a were calculated by dividing

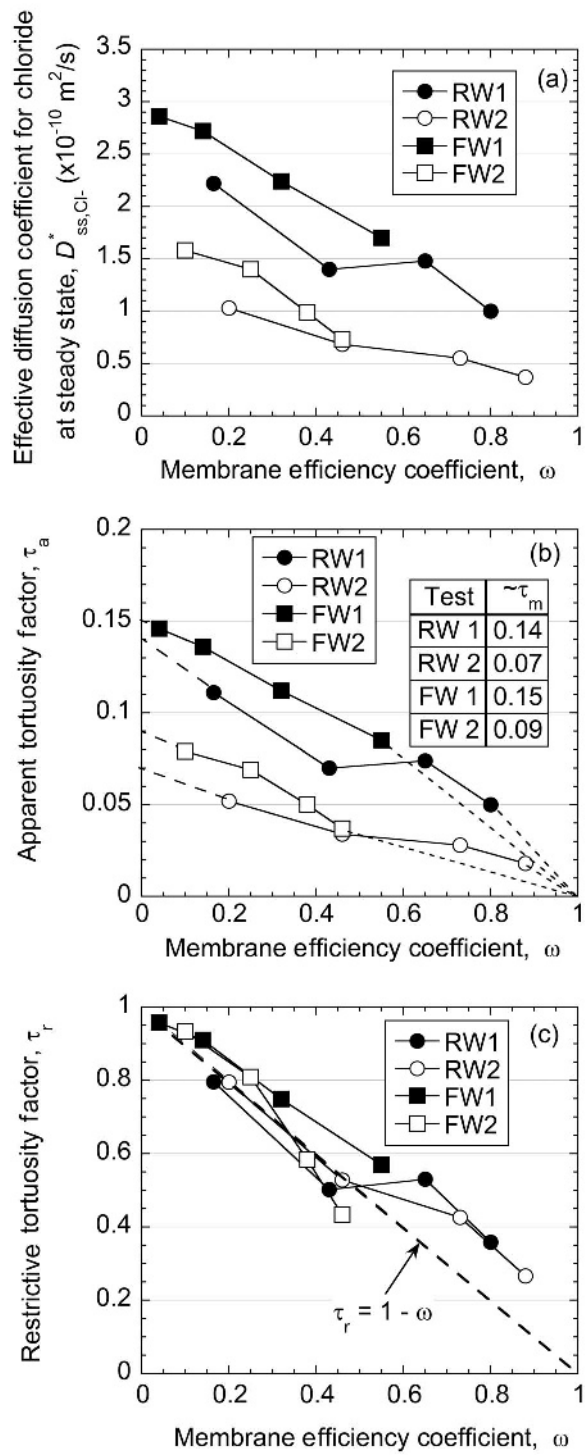

Figure 10. Steady-state effective diffusion coefficients and tortuosity factors for diffusion of chloride (Cl^-) through bentonite-polymer composite (BPC) based on rigid-wall (RW) and flexible-wall (FW) test results as a function of membrane efficiency: (a) effective diffusion coefficients; (b) apparent tortuosity factors; (c) restrictive tortuosity factors [τ_m = matrix tortuosity factor].

https://doi.org/10.1346/CCMN.2015.0630301 Published online by Cambridge University Press

the values of D^*_{ss,Cl^-} by the free-solution (aqueous-phase) diffusion coefficient, D_o, for KCl of 19.93×10^{-10} m^2/s (Shackelford and Daniel, 1991). The resulting values of τ_a (Figure 10b) varied from 0.14 for test FW1 to 0.017 for test RW2. The values of τ_a were lower for tests RW2 and FW2 relative to those for tests RW1 and FW1. This difference occurs because tests RW2 and FW2 were conducted at lower porosities and higher σ' values, respectively, resulting in more tortuous pathways.

Because D^* is a function of ω (Figure 10a) and τ_a (equation 4), τ_a must also be a function of ω (Figure 10b). That is, as ω approaches unity, τ_a must approach zero because, by definition, an ideal or perfect semipermeable membrane ($\omega = 1$) is one in which all solutes are restricted from migration. In addition, τ_a approaches a maximum value representing the matrix tortuosity factor, τ_m, as ω approaches zero (*i.e.* $\tau_a \rightarrow \tau_m$ as $\omega \rightarrow 0$). As a result, values of τ_m were estimated by extrapolating the trends in the τ_a *vs.* ω data, and the resulting values of τ_m are tabulated within Figure 10b. The lowest value for τ_m of ~0.07 occurred for test RW2, whereas the values of τ_m for tests RW1 and FW1 were similar at 0.14 and 0.15, respectively.

As noted previously, τ_a is also defined as the product of τ_m and τ_r (equation 5). Values of τ_r were therefore calculated as the ratio of τ_a relative to τ_m, or τ_a/τ_m (Malusis and Shackelford, 2002b). The resulting values of τ_r (Figure 10c) tend to decrease as ω increases. This trend of decreasing τ_r with increasing ω is due to a more restrictive migration pathway resulting from an increased solute restriction and/or viscosity of water due to a thicker diffuse double layer (Shackelford and Daniel, 1991; Malusis and Shackelford, 2002b; Malusis *et al.*, 2013; Shackelford and Moore, 2013; Malusis *et al.*, 2014). In addition, the values of τ_r were lower for both rigid-wall tests (RW1 and RW2) and the flexible-wall test conducted at the higher σ' values (FW2), indicating that the migration pathways for these tests were more restrictive than those for test FW1. Based largely on the results presented by Malusis and Shackelford (2002b), Manassero and Dominijanni (2003) proposed that τ_r be estimated using the correlation, $\tau_r = 1 - \omega$. The values of τ_r for the present study generally followed this linear correlation with ω (Figure 10c).

Comparison of BPC vs. traditional Na-bentonite

The values of D^*_{ss,Cl^-} measured in the present study for the BPC can be compared with those reported previously by Malusis and Shackelford (2002b) for a GCL containing a traditional Na-bentonite (Figure 11). The values of D^*_{ss,Cl^-} for the BPC measured in this study were similar to those for the GCL containing a traditional Na-bentonite, except for the results from test RW2, where the D^*_{ss,Cl^-} values for the BPC ranged from 3.7×10^{-11} to 1.0×10^{-10} m^2/s for C_{ot} ranging from 4.7 to 54 mM KCl, respectively, whereas the D^*_{ss,Cl^-} values for the GCL ranged from 7.1×10^{-11} to 2.3×10^{-10} m^2/s for C_{ot} ranging from 3.9 to 47 mM KCL, respectively (Figure 11a). The lower D^*_{ss,Cl^-} value for test RW2 correlated with the higher ω for the BPC relative to that for the GCL. The lower D^*_{ss,Cl^-} and higher ω for the BPC relative to the GCL with similar porosities (0.80 for the BPC *vs.* 0.78–0.80 for the GCL) indicate that other factors contributed to the measured D^*_{ss,Cl^-} and ω of the BPC, possibly the polymer (PAA) clogging the pores of the BPC (Scalia *et al.*, 2011; Scalia, 2012; Bohnhoff and Shackelford, 2013; Scalia *et al.*, 2014).

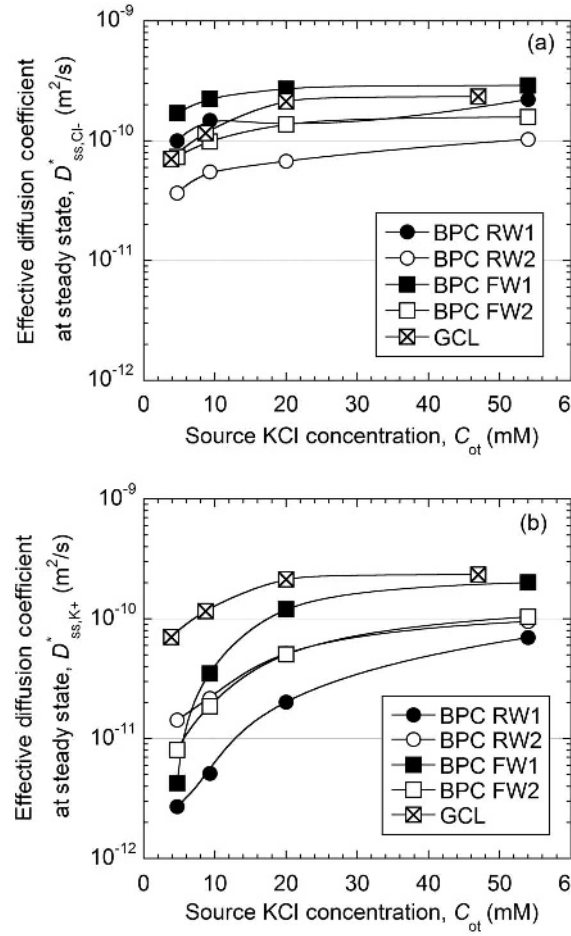

Figure 11. Comparison of the effective diffusion coefficients at steady state for bentonite polymer-composite (BPC) *vs.* a geosynthetic clay liner (GCL) reported by Malusis and Shackelford (2002b) as a function of source KCl concentration: (a) chloride; (b) potassium [RW = rigid-wall test; FW = flexible-wall test].

In contrast, the values D^*_{ss,K^+}, measured in the present study for the BPC were much lower than those for the GCL, especially at lower C_{ot} (*e.g.* < 20 mM KCl; Figure 11b). The values of D^*_{ss,K^+} for the GCL varied from 4.4×10^{-11} to 2.0×10^{-10} m^2/s, whereas the values of D^*_{ss,K^+} for the BPC varied from 2.7×10^{-12} m^2/s for test RW1 to 2.0×10^{-10} m^2/s for test FW1. The lower values of D^*_{ss,K^+} for the BPC relative to those for the GCL can be attributed, in part, to the likely larger

https://doi.org/10.1346/CCMN.2015.0630301 Published online by Cambridge University Press

amounts of remnant Na^+ in the BPC relative to the GCL (*i.e.* non-flushed BPC *vs*. flushed GCL), resulting in the aforementioned requirement for electroneutrality in diffusive charge flux and the lack of achieving true steady state diffusion for K^+ due to cation exchange with Na^+.

In general, the value of τ_m decreased with decreasing n for the BPC (Figure 12). The trend of τ_m *vs*. n was linear over the narrow range in porosities encountered in the present study (*i.e.* $0.80 \leqslant n \leqslant 0.95$). However, the negative y intercept suggests that the relationship between τ_m and n was non-linear overall. In contrast, the τ_m for the GCL containing traditional Na-bentonite (Figure 12) was significantly greater than that for BPC at a similar porosity ($\tau_m = 0.12$ @ $n = 0.79$ and $\tau_m = 0.07$ @ $n = 0.80$, respectively). Because τ_m represents the component of the apparent tortuosity attributed only to the geometry of interconnected pores, a lower τ_m value for the BPC at similar n indicates that the diffusive pathways of the interconnected pores for the BPC were more tortuous than those for the GCL due, in part, to the presence of the polymer in the pores of the BPC (Bohnhoff and Shackelford, 2013; Scalia *et al.*, 2014).

SUMMARY AND CONCLUSIONS

The present study evaluated the diffusion of a simple salt, KCl, through a bentonite-polymer composite (BPC) that is known to behave as a semipermeable membrane for the conditions imposed in the study. Aside from representing the first evaluation of salt diffusion through a BPC reported in the literature, the results presented here are unique relative to previous studies in two other ways, *i.e.* the specimens of the BPC evaluated here were not flushed (leached) of soluble salts prior to testing, resulting in an initial excess of soluble salts, primarily Na^+ within the pore liquid of the specimens, and multiple-stage rather than single-stage tests were conducted.

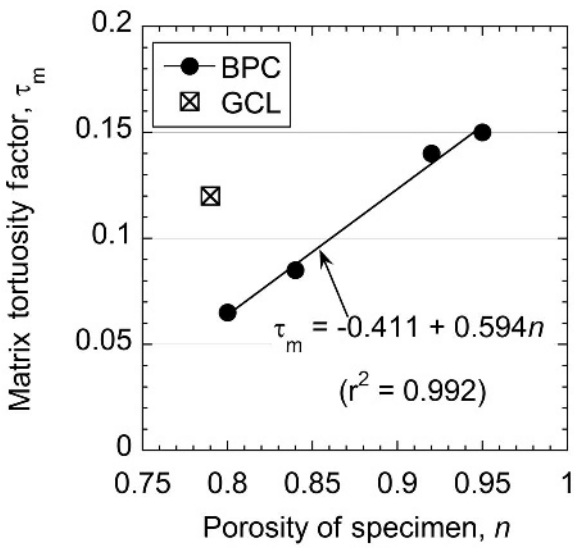

Figure 12. Matrix tortuosity factor *vs.* specimen porosity for the bentonite-polymer composite (BPC) evaluated in this study *vs.* that for a geosynthetic clay liner (GCL) previously reported by Malusis and Shackelford (2002b).

Similar to previously reported results for diffusion of KCl through a traditional Na-bentonite contained within a GCL, the effective diffusion coefficients, D^*, of both Cl^- and K^+ decreased with increasing membrane efficiency coefficient, ω, of the BPC, and the decrease in D^* correlated approximately with the quantity $(1 - \omega)$. This trend is consistent with the requirement that solute diffusion must approach zero in the limit as membrane efficiency approaches unity (*i.e.* $D^* \rightarrow 0$ as $\omega \rightarrow 1$), *i.e.* because by definition no solutes can pass through an ideal membrane ($\omega = 1$). Thus, polymerization of the bentonite did not significantly affect the expected correlation between D^* and ω based on the previous results shown for flushed specimens of a traditional (unmodified) Na-bentonite.

Unlike previously reported results for diffusion of KCl through traditional Na-bentonite, wherein the steady-state values of D^* for Cl^-, D^*_{ss,Cl^-}, were almost identical to those for those for K^+, D^*_{ss,K^+}, at all values of the source concentration of KCl, C_{ot}, D^*_{ss,Cl^-} for the BPC in this study was always greater than D^*_{ss,K^+}, with the differences between D^*_{ss,Cl^-} and D^*_{ss,K^+} decreasing with increasing C_{ot} of KCl. This difference in results was attributed to the predominance of excess Na^+ initially within the pores of the specimens of the BPC, and the electroneutrality requirement for charge flux balance at steady state. That is, at the lower magnitudes of C_{ot}, a greater percentage of the charge flux balance was carried by the diffusion of remnant Na^+ through both the top and bottom of the specimen, but this contribution to the charge flux balance diminished with increasing time due to the diminishing concentration of remnant Na^+ initially contained within the pore liquid and the increasing dominance of K^+ resulting from increasing C_{ot}.

A comparison of the diffusive mass fluxes at steady state for Cl^- *vs.* K^+ indicated that the K^+ had not actually achieved steady state diffusion due to continual cation exchange with Na^+, despite values of r^2 associated with the apparent steady state data for K^+ being close to unity ($\geqslant 0.996$). As a result, values of D^*_{ss,K^+} for the BPC in this study were typically lower than those reported for specimens of a traditional Na-bentonite that was flushed of remnant Na^+ prior to testing, especially at the lower values of C_{ot}. However, values of D^*_{ss,Cl^-} for the BPC evaluated in this study were similar to those reported previously for the traditional Na-bentonite, as expected on the basis that Cl^-, a non-reactive tracer, was the dominant anion species in both studies. Thus, whether or not the specimens were flushed of soluble salts prior to testing does not appear to have a significant impact on the steady-state diffusion of the dominant anionic species, all other factors being equal.

https://doi.org/10.1346/CCMN.2015.0630301 Published online by Cambridge University Press

ACKNOWLEDGMENTS

Financial support for this project, a collaboration among Colorado State University, the University of Wisconsin-Madison (UW-Madison), and Colloid Environmental Technologies Co. (CETCO), was provided by the U.S. National Science Foundation (NSF), Arlington, Virginia, under Grant No. CMMI-0757815. The opinions expressed in this paper are solely those of the authors and are not necessarily consistent with the policies or opinions of the NSF. The authors thank CETCO for providing the bentonites used in this study, the assistance of all the collaborators including Joe Scalia, Craig Benson, and Tuncer Edil at UW-Madison and Mike Donovan and Jerry Darlington of CETCO. The authors also appreciate the assistance of Kristin Sample-Lord, Catherine Hong, and Jong Beom Kang of CSU in conducting the tests. Finally, the assistance of Dr Thomas Borch of CSU in conducting anion concentration analyses by ion chromatography is appreciated.

REFERENCES

Ashmawy, A., Darwish, E., Sotelo, N., and Muhammad, N. (2002) Hydraulic performance of untreated and polymer-treated bentonite in inorganic landfill leachates. *Clays and Clay Minerals*, **50**, 546–552.

Boels, D. and van der Wal, K. (1999) Trisoplast: New developments in soil protection. Sardinia 99, CISA, Caligari, Italy, pp. 77–84.

Bohnhoff, G. (2012) Membrane behavior, diffusion, and compatibility of a polymerized bentonite for containment barrier applications. PhD dissertation, Colorado State University, Fort Collins, Colorado, USA.

Bohnhoff, G. and Shackelford, C. (2013) Improving membrane performance via bentonite polymer nanocomposite. *Applied Clay Science*, **86**, 83–98.

Christman, M., Benson, C., and Edil, T. (2002) Geophysical evaluation of annular well seals. *Ground Water Monitoring and Remediation*, **22**, 104–112.

Crank, J. (1975). *The Mathematics of Diffusion*, 2nd edition. Clarendon Press, Oxford, England.

Di Emidio, G. (2010) Hydraulic and chemico-osmotic performance of polymer treated clay. PhD dissertation, University of Ghent, Belgium.

Di Emidio, G., van Impe, P., and Mazzieri, F. (2010) A polymer enhanced clay for impermeable geosynthetic clay liners. *Sixth International Conference on Environmental Geotechnics*, Tata McGraw Hill, New Delhi, India, pp. 963–967.

Di Emidio, G., van Impe, P., and Flores, V. (2011) Advances in geosynthetic clay liners: polymer enhanced clays. *GeoFrontiers 2011: Advances in Geotechnical Engineering* (J. Han and D. Alzamora, editors), ASCE, Reston, Virginia, USA, pp. 1931–1940.

Dominijanni, A. and Manassero, M. (2012a) Modelling the swelling and osmotic properties of clay soils. Part I: The phenomenological approach. *International Journal of Engineering Science*, **51**, 32–50.

Dominijanni, A. and Manassero, M. (2012b) Modelling the swelling and osmotic properties of clay soils. Part II: The physical approach. *International Journal of Engineering Science*, **51**, 51–73.

Dominijanni, A., Manassero, M., and Puma, S. (2013) Coupled chemical-hydraulic-mechanical behaviour of bentonites. *Geotechnique*, **63**, 191–205.

Estornell, P. and Daniel, D.E. (1992) Hydraulic conductivity of three geosynthetic clay liners. *Journal of Geotechnical Engineering*, **118**, 1592–1606.

Evans, J. (1994) Hydraulic conductivity of vertical cutoff walls. Pp. 79–94 in: *Hydraulic Conductivity and Waste Contaminant Transport in Soil* (D.E. Daniel and S. Trautwein, editors), ASTM, West Conshohocken, Pennsylvania, USA.

Gleason, M., Daniel, D., and Eykholt, G. (1997) Calcium and sodium bentonite for hydraulic containment applications. *Journal of Geotechnical and Geoenvironmental Engineering*, **123**, 438–445.

Heller, H. and Keren, R. (2003) Anionic polyacrylamide polymer adsorption by pyrophyllite and montmorillonite. *Clays and Clay Minerals*, **51**, 334–339.

Jo, H., Benson, C., Shackelford, C., Lee, J-M., and Edil, T. (2005) Long-term hydraulic conductivity of a geosynthetic clay liner permeated with inorganic salt solutions. *Journal of Geotechnical and Geoenvironmental Engineering*, **131**, 405–417.

Kajita, L. (1997) An improved contaminant resistant clay for environmental clay liner applications. *Clays and Clay Minerals*, **45**, 609–617.

Kang, J. and Shackelford, C. (2009) Clay membrane testing using a flexible-wall cell under closed-system boundary conditions. *Applied Clay Science*, **44**, 43–58.

Kang, J. and Shackelford, C. (2011) Consolidation enhanced membrane behavior of a geosynthetic clay liner. *Geotextiles and Geomembranes*, **29**, 544–556.

Kolstad, D., Benson, C., and Edil, T. (2004) Hydraulic conductivity and swell of non-prehydrated geosynthetic clay liners permeated with multispecies inorganic solutions. *Journal of Geotechnical and Geoenvironmental Engineering*, **130**, 1236–1249.

Lagaly, G., Ogawa, M., and Dékány, I. (2006) Clay mineral organic interactions. Pp. 309–377 in: *Handbook of Clay Science* (F. Bergaya, B.K.G. Theng, and G. Lagaly, editors). Developments in Clay Science, Elsevier, Amsterdam.

Malusis, M. and Shackelford, C. (2002a) Chemico-osmotic efficiency of a geosynthetic clay liner. *Journal of Geotechnical and Geoenvironmental Engineering*, **128**, 97–106.

Malusis, M. and Shackelford, C. (2002b) Coupling effects during steady-state solute diffusion through a semipermeable clay membrane. *Environmental Science & Technology*, **36**, 1312–1319.

Malusis, M., Shackelford, C., and Olsen, H. (2001) A laboratory apparatus to measure chemico-osmotic efficiency coefficients for clay soils. *Geotechnical Testing Journal*, **24**, 229–242.

Manassero, M. and Dominijanni, A. (2003) Modelling the osmosis effect on solute migration through porous media. *Geotechnique*, **53**, 481–492.

Malusis, M., Kang, J., and Shackelford, C. (2013) Influence of membrane behavior on solute diffusion through GCLs. Pp. 267–242 in: *Coupled Phenomena in Environmental Geotechnics* (M. Manassero, A. Dominijanni, S. Foti, and G. Musso, editors). CRC Press/Balkema, Taylor & Francis Group, London.

Malusis, M., Kang, J., and Shackelford, C. (2014) Restricted salt diffusion in a geosynthetic clay liner. *Environmental Geotechnics*, **2**, 68–77.

Mazzieri, F. (2011) Impact of desiccation and cation exchange on the hydraulic conductivity of factory-prehydrated GCLs. Pp. 976–985 in: *GeoFrontiers 2011: Advances in Geotechnical Engineering* (J. Han and D. Alzamora, editors). ASCE, Reston, Virginia, USA.

Mazzieri, F., Di Emidio, G., and Van Impe, P. (2010a) Diffusion of calcium chloride in a modified bentonite: impact on osmotic efficiency and hydraulic conductivity. *Clays and Clay Minerals*, **58**, 351–363.

Mazzieri, F., Pasqualini, E., and Di Emidio, G. (2010b)

Migration of heavy metals through conventional and factory-prehydrated GCL materials. Pp. 960–963 in: *Sixth International Conference on Environmental Geotechnics*. Tata McGraw Hill, New Delhi, India.

Muzny, C., Butler, B., Hanley, H., Tsvetkov, F., and Peiffer, D. (1996) Clay platelet dispersion in a polymer matrix. *Materials Letters*, **28**, 379–384.

Onikata, M., Kondo, M., and Kamon, M. (1996) Development and characterization of a multiswellable bentonite. Pp. 587–590 in: *2nd International Congress on Environmental Geotechnics* (M. Kamon, editor), A.A. Balkema, Rotterdam, The Netherlands.

Onikata, M., Kondo, M., Hayashi, N., and Yamanaka, S. (1999) Complex formation of cation-exchanged montmorillonites with propylene carbonate: Osmotic swelling in aqueous electrolyte solutions. *Clays and Clay Minerals*, **47**, 672–677.

Scalia, J. (2012) Bentonite-polymer composites for containment applications. PhD dissertation, University of Wisconsin-Madison, Madison, Wisconsin, USA.

Scalia, J., Benson, C., Edil, T., Bohnhoff, G., and Shackelford, C. (2011) Geosynthetic clay liners containing bentonite polymer nanocomposite. Pp. 2001–2009 in: *GeoFrontiers 2011: Advances in Geotechnical Engineering* (J. Han and D. Alzamora, editors). ASCE, Reston, Virginia, USA.

Scalia, J., Benson, C.H., Bohnhoff, G., Edil, T., and Shackelford, C. (2014) Long-term hydraulic conductivity of a bentonite-polymer composite permeated with aggressive inorganic solutions. *Journal of Geotechnical and Geoenvironmental Engineering*, **140**, 04013025-1-04013025-13.

Shackelford, C. (1991) Laboratory diffusion testing for waste disposal – A review. *Journal of Contaminant Hydrology*, **7**, 177–217.

Shackelford, C. (2011) Membrane behavior in geosynthetic clay liners. Pp. 1961–1970 in: *GeoFrontiers 2011: Advances in Geotechnical Engineering* (J. Han and D. Alzamora, editors). ASCE, Reston, Virginia, USA.

Shackelford, C. (2012) Membrane behavior of engineered clay barriers for geoenvironmental containment: State of the art. Pp. 3419–3428 in: *GeoCongress 2012–State of the Art and Practice in Geotechnical Engineering* (R. Hryciw, A. Athanasopoulos-Zekkos, and N. Yesiller, editors). ASCE, Reston, Virginia, USA.

Shackelford, C. (2013) Membrane behavior in engineered bentonite-based containment barriers: State of the art. Pp. 45–60 in: *Coupled Phenomena in Environmental Geotechnics* (M. Manassero, A. Dominijanni, S. Foti, and G. Musso, editors). CRC Press/Balkema, Taylor & Francis Group, London.

Shackelford, C., Benson, C., Katsumi, T., Edil, T., and Lin, L. (2000) Evaluating the hydraulic conductivity of GCLs permeated with non-standard liquids. *Geotextiles and Geomembranes*, **18**, 133–161.

Shackelford, C. and Daniel, D. (1991) Diffusion in saturated soil. 1. Background. *Journal of Geotechnical Engineering*, **117**, 467–484.

Shackelford, C. and Lee, J. (2003) The destructive role of diffusion on clay membrane behavior. *Clays and Clay Minerals*, **51**, 186–196.

Shackelford, C. and Moore, S. (2013) Fickian diffusion of radionuclides for engineered containment barriers: Diffusion coefficients, porosities, and complicating issues. *Engineering Geology*, **152**, 133–147.

Shackelford, C. and Sample-Lord, K. (2014) Hydraulic conductivity and compatibility of bentonite for hydraulic containment applications. Pp. 370–387 in: *From Soil Behavior Fundamentals to Innovations in Geotechnical Engineering* (M. Iskander, J. Garlanger, and M. Hussein, editors). Geotechnical Special Publication **233** honoring Roy E. Olson, ASCE, Reston, Virginia, USA.

Shackelford, C., Malusis, M., and Olsen, H. (2003) Clay membrane behavior for geoenvironmental containment. Pp. 767–774 in: *Soil and Rock America Conference 2003, vol. 1* (P. Culligan, H. Einstein, and A. Whittle, editors). Verlag Glückauf GMBH, Essen, Germany.

Skagius, K. and Neretnieks, I. (1986) Porosities and diffusivities of some non-sorbing species in crystalline rocks. *Water Resources Research*, **22**, 389–398.

Smith, J., Bartelt-Hunt, S., and Burns, S. (2003) Sorption and permeability of gasoline hydrocarbons in organobentonite porous media. *Journal of Hazardous Materials*, **96**, 91–97.

Trauger, R. and Darlington, J. (2000) Next generation geosynthetic clay liners for improved durability and performance. 14th GRI Conference, Geosynthetic Institute, Folsom, Pennsylvania, USA, pp. 255–267.

(*Received 17 January 2014; revised 21 April 2015; Ms. 837; AE: W.F. Jaynes*)